Semiconductor Physics, Quantum Electronics & Optoelectronics, 2009. V. 12, N 1. P. 68-71.

PACS 72.20.Pa, 77.84.Bw

Effect of Si infiltration method on the properties of biomorphous SiC

V.S. Kiselov*, E.N. Kalabukhova, A.A. Sitnikov, P.M. Lytvyn, V.I. Poludin, V.O. Yukhymchuk, A.E. Belyaev
V. Lashkaryov Institute of Semiconductor Physics, NAS of Ukraine
41, prospect Nauky, 03028 Kyiv, Ukraine
**Corresponding author – fax: 38 (044)-525-59-40; e-mail: vit_kiselov@ukr.net*

Abstract. Two types of wood-based biomorphous SiC composites with different microstructure were obtained by infiltration of carbon template with liquid or vapour silicon. The oak, pine, lilac, walnut, acacia woods available in Ukraine were used as the biological template in this work. SEM, optical and AFM data indicated that biomorphous SiC obtained by melt infiltration consists of crystalline phase of 3C-SiC, while that of vapor infiltration results in formation of crystalline and amorphous phases of 3C-SiC. The same results were obtained for infiltration of carbon fibers. Thus, it was suggested that the mechanism of SiC formation is governed by the infiltration method.

Keywords: biomorphous SiC, Si infiltration, SEM, AFM, EPR, Raman scattering.

Manuscript received 11.12.08; accepted for publication 18.12.08; published online 02.03.09.

1. Introduction

Biomorphous composites SiC/Si are known in the literature as ecoceramics – environment conscious ceramics [1-3]. Among the biomorphous composites, the porous SiC ceramics has been considered to be as one of the best candidate materials for orthopedic and dental implants due to their high level of biocompatibility, chemical inertness and mechanical strength [4-6]. Porous SiC has also a great potential for many industrial applications such as light ultra strong material in aerospace and motor-car industry, as well as a heat insulation material due to the low thermal expansion coefficient, small value of the relative density, mechanical strength, high chemical inertness, oxidation and corrosion resistance.

The objective of this work is to examine the effect of infiltration method on the parameters of wood-based biomorphous SiC composites. For this purpose, the biomorphous SiC was fabricated by infiltration of the carbon template with liquid or vapor silicon (Si).

2. Technology preparation

The technology process of biomorphous SiC preparation is well known [1-3]. The developed processing scheme for manufacturing the wood-based biomorphous SiC composite by the infiltration method used in this work is shown in Fig. 1.

The oak, pine, lilac, walnut, acacia woods available in Ukraine with average dimensions of 20-40 mm in diameter and height of 12 mm were used as the biological template in this study. At the initial stage, wood samples were pyrolized at 900 °C in an argon atmosphere. After pyrolysis, the carbon templates were reacted with liquid or vapour silicon produced by melting Si powder at 1500 °C in a graphite crucible in inert (Ar) atmosphere. For this purpose, the resistive furnace (REDMET 30) with graphite crucible was used. The carbon templates were placed into the graphite crucible along with well-milled Si. The Si/C/ ratio was of $\psi = 2$. Design of the graphite crucible allows fixing the position of the carbon templates so that only half of the carbon template was immersed into the Si melt providing the infiltration of that both with liquid and vapor Si.

The spontaneous Si infiltration of the carbon templates was performed at 1500-1600 °C for 10-15 min in inert atmosphere (Ar or He). After that, the temperature was raised up to 1800-1900 °C and held for 30-60 min. The final material of the reaction was a SiC/C composite with a wood-like microstructure. An excess carbon was burn out in furnace in oxygen atmosphere at 900 °C for 2 hours.

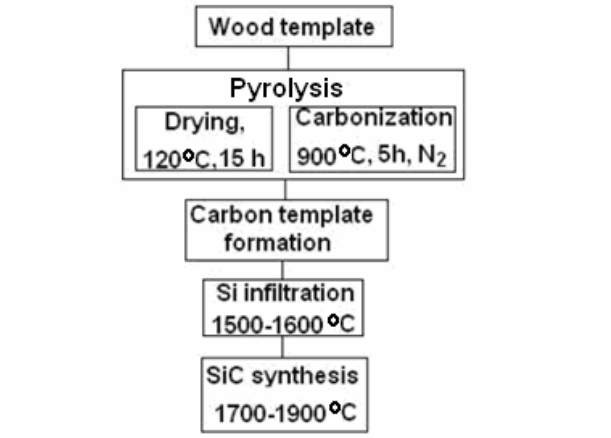

Fig. 1. Processing scheme for manufacturing biomorphous SiC.

3. Experimental results and discussion

Optical and scanning electron microscopy (SEM), atomic force microscopy, Raman scattering spectroscopy and electron paramagnetic resonance (EPR) were used for compositional and structural analysis of biomorphous SiC.

Surface and transverse cross section of the template were studied by SEM after infiltration and siliconization. Fig. 2 shows images of the transverse cross section of biomorphous SiC grown from walnut.

It was established that the mechanical properties, structure and color of biomorphous SiC depend on the carbon template infiltration method. The melt infiltration resulted in final material with high mechanical strength and green-brown color which was labeled as SiC-1 (see Fig. 2b), while the infiltration with Si vapor resulted in final material of white color with fibrous structure and was labeled as SiC-2 (see Fig. 2c). It was also found that the type of infiltration (with liquid or vapor Si) depends on wood species. The fibrous structure of SiC-2 was clearly demonstrated when excess carbon was burn out. The fiber diameter is determined by tubular pore sizes in carbon template and varies from 1 to 30 μm. The fibers have a low mechanical strength and could be easily separated from the carbon template walls.

As it is seen from Figs 3 and 4, the fibers have flaked structure and ultrasonic treatment easily separates the flakes.

Raman spectra (RS) were taken with double grating spectrometer DFS-24 at room temperature. The 514.5-nm line of an Ar^+-laser was used for the excitation. The signal was registered with a cooled phototube working in photon counting mode in back scattering geometry. Fig. 5 shows RS observed in two types of biomorphous SiC grown from lilac. Analysis of RS peak frequencies observed in biomorphous SiC shows that biomorphous SiC-1 should be attributed to the 3C polytype. Slightly higher values of LO and TO phonon bands (TO – 796 cm^{-1} and LO – 972 cm^{-1}) with respect to those in

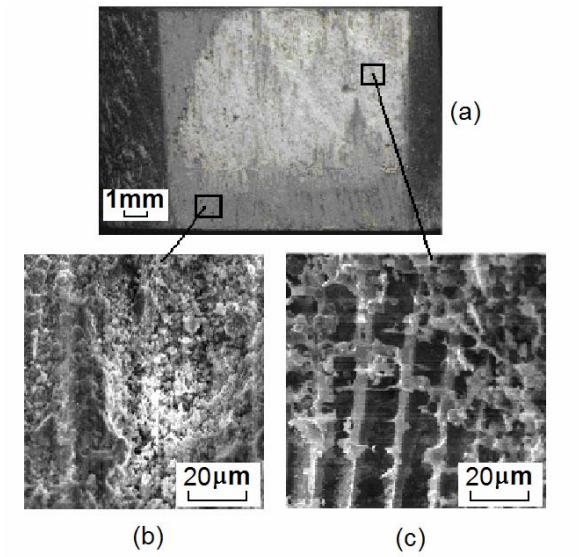

Fig. 2. Photo (a) and SEM images (b, c) of the transverse section of biomorphous SiC grown from walnut.

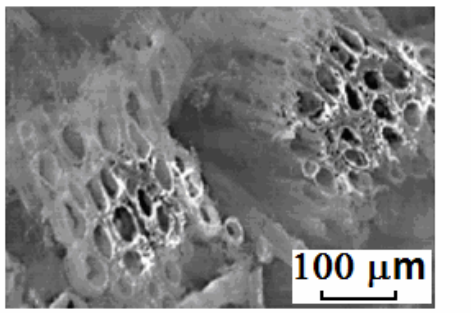

Fig. 3. Optical microscopy image of tubular fiber packages of the biomorphous SiC grown from lilac.

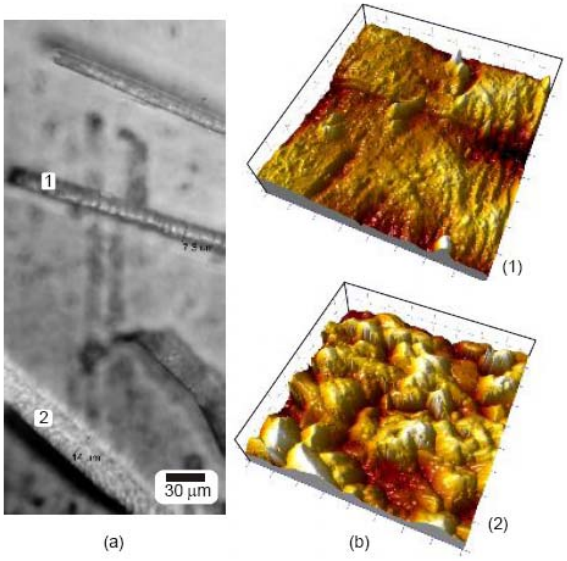

Fig. 4. Photomicrography (a) and AFM image (b) of SiC fibers grown from pine with scan size of 4×4 μm and Z-range of 0.1 μm.

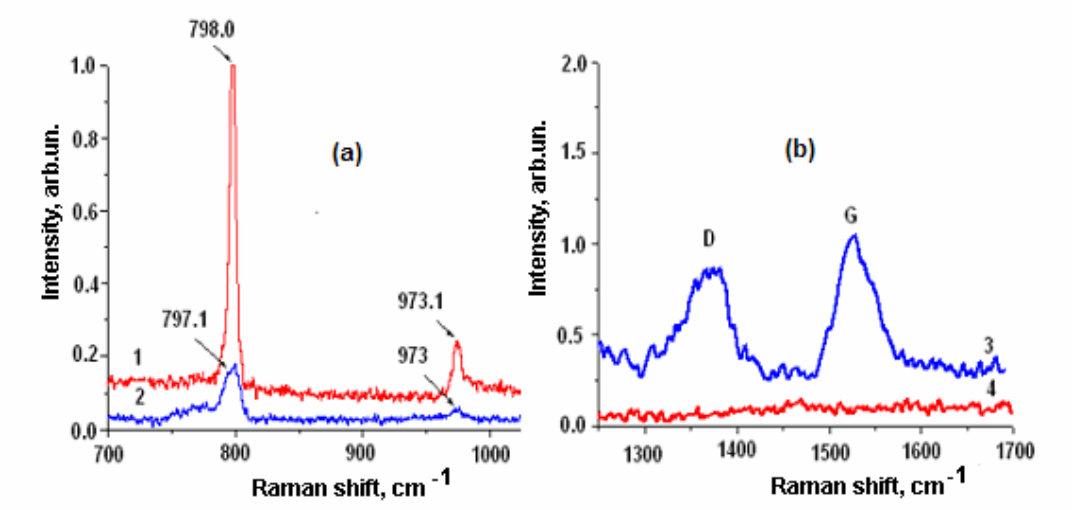

Fig. 5. RS of SiC-1 and SiC-2: a) RS of SiC observed in the C-C oscillation range, *1* – SiC-1, *2* – SiC-2, b) RS of SiC-1 observed in the 1300-1700 cm^{-1} range, *3* – as-synthesized SiC-1, *4* – carbon excess was burn out from SiC-1.

crystalline 3C-SiC indicate that the biomorphous SiC is affected by compression. The LO and TO phonon bands in RS of SiC-2 have lower intensities than in SiC-1. In addition, the broad band centred at 765 cm^{-1} was observed in RS of SiC-2 and could be attributed to the amorphous phase of SiC [7, 8]. Thus, SiC-2 consists of crystalline and amorphous phase of 3C-SiC. It should be noted that depending on the SiC technology treatment the disordered (D) and graphitic (G) bands were observed in RS of SiC-1 (see Fig. 5b) due to clusters of carbon spots [9] which disappeared when excess carbon was burn out.

EPR spectrum was measured at 77 K and 9 GHz. In all the samples under EPR investigation, excess carbon was burnt out in oxygen atmosphere at 900°C. The spectrum of biomorphous SiC-2 with fibrous structure is shown in Fig. 6. There present is the 0.3 mT wide single resonance with $g = 2.0023 \pm 0.0002$, which is closer to the free electron value (2.0023) than to the usual carbon related EPR center value (2.0028) observed in amorphous carbon [10] and amorphous SiC material [11]. The fact that the *g*-value of the defect is closed to the free electron one indicates that unpaired electrons of carbon related defect in amorphous phase of SiC-2 are delocalized due to formation of the carbon clusters. On the other hand, considering that SiC-2 contains crystalline phase of 3C-SiC, the observed EPR signal could be attributed to the carbon dangling bonds in crystalline phase of 3C-SiC. Our previous study of 3C-SiC powders was shown that the *g*-factor of carbon dangling bonds in polycrystalline 3C-SiC have $g = 2.0023$ [12]. But in the light of the fact that EPR signal was not observed in SiC-1 containing only crystalline phase of 3C-SiC the first interpretation of the paramagnetic defect seems to be more plausible.

In order to determine the reaction mechanisms governing siliconization of carbon, we additionally applied impregnation of carbon fiber samples from the liquid or gas-phase of silicon. A SEM image of carbon fiber bunches after their processing are shown in Fig. 7. Faceted micro-crystals of the β-SiC (size 4-5 μm) are observed on fibers in the case of liquid silicon

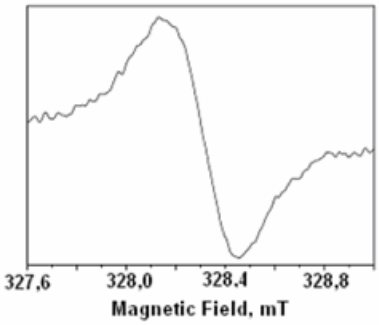

Fig. 6. EPR spectrum recorded at 9 GHz and 77 K in biomorphous SiC-2.

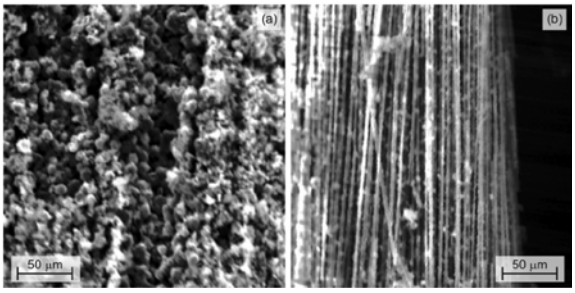

Fig. 7. SEM images of carbon fibers after SiC synthesis using liquid silicon (a) or its vapor (b).

infiltration. These results are confirmed by the results obtained in [13, 14]. Therefore, it could be suggested that the formation of the SiC precipitates are caused by the process of carbon dissolution in liquid Si (model via solution-precipitation) [15, 16]. The infiltration with vapor Si resulted in smooth-faced, unstructured fibers consisting of amorphous SiC possibly due to the diffusion-controlled process [17, 18]. Comparatively weak diffuse mass transport of Si takes place at gas-phase infiltration, and only a thin layer of amorphous SiC is formed. These materials have different colors. Materials with microcrystalline structure have yellow-brown coloration and amorphous layers have white coloration.

4. Conclusion

The growth technology and parameters of wood-based biomorphous SiC ceramics obtained by infiltration with liquid or vapor silicon were examined. The relationship between infiltration method and microstructure of biomorphous SiC was established. It was found that structure and phase composition of the material depend on the carbon template infiltration method. Optical, EPR and SEM data indicate that the melt infiltration results in biomorphous SiC with crystalline phase of 3C-SiC with the faceted morphology, while infiltration with Si vapor results in SiC with fibrous structure are provides both crystalline and amorphous phases of 3C-SiC. Thus, it was suggested that the mechanism of SiC formation is governed by the infiltration method.

References

1. P. Greil, T. Lifka, A. Kaindl // *J. Europ. Ceram. Soc.* **18**, p. 1975-1983 (1998).
2. F.M. Varela-Feria, J. Martinez-Fernandez, A.R. de Arellano-Lopez, M. Singh // *J. Europ. Ceram. Soc.* **22**, p. 2719-2725 (2002).
3. M. Presas, J.Y. Pastor, J. Llorca, A.R. Arellano Lopez, J. Martinez Fernandez, R. Sepulveda // *Intern. J. Refractory Metals & Hard Materials* **24**, p. 49-54 (2006).
4. S. Santavirta, M. Takagi, L. Nordsletten, A. Anttila, R. Lappalainen, Y.T. Konttinen // *Arch Orthop. Trauma Surg.* **118** (1-2), p. 89-91 (1998).
5. L. Nordsletten, A.K.M. Hogasen, Y.T. Konttinen, S. Santavirta, P. Aspenberg, A.O. Aasen // *Biomaterials* **17**, p. 1521-1527 (1996).
6. A. de Carlos, J.P. Borrajo, J. Serra, P. Gonzalez, B. Leon // *J. Mater. Sci.: Mater. Med.* **17**, p. 523-529 (2006).
7. *Properties of Silicon Carbide*, edited by Gary L. Harris. IEE, INSPEC, the Institution of Electrical Engineers, London, 1995.
8. S. Klein, L. Houben, R. Carius, F. Finger, W. Fischer // *J. Non-Crystal. Solids* **352**, p. 1376-1379 (2006).
9. J. Robertson, Amorphous carbon // *Advanced in Physics* **35**, No. 4, p. 317-374 (1986).
10. H.J. von Bardeleben, J.L. Cantin, K. Zellama, A. Zeinert // *Diamond and Related Materials* **12**, p. 124-129 (2003).
11. T. Christidis, M. Tabbal, S. Isber, M.A. El Khakani, M. Chaker // *Appl. Surf. Sci.* **184**, p. 268-272, 2001.
12. E.N. Kalabukhova, S.N. Lukin and O.T. Sergeev // *Fizika Tverd. Tela* **35**, p. 408 (1993) (in Russian)
13. C. Zollfrank, H. Sieber, Microstructure evolution and reaction mechanism of biomorphous SiSiC ceramics // *J. Amer. Ceram. Soc.* **88**(1), p. 51-58 (2005).
14. M. Pyzalski, J. Bialoskorski, E. Walasek, Reaction between carbon fibres and molten silicon: heat determination using DTA // *J. Therm. Anal.* **31**, p. 1193-1196 (1986).
15. R. Pampuch, E. Walasek, J. Bialoskorski, Mechanism of reactions in Si_l+C_f system // *Ceram. Int.* **13**(1), p. 63-68 (1987).
16. P. Greil, T. Lifkaand, A. Kaindl, Biomorphic cellular silicon carbide ceramics from wood // *J. Europ. Ceram. Soc.* **18**(14), p. 1961-1973 (1998).
17. E. Fitzer, R. Gadow, Fibre reinforced silicon carbide // *Amer. Ceram. Soc. Bull.* **65**(2), p. 326-335 (1986).
18. H. Zhou, R.N. Singh, Kinetics model for the growth of silicon carbide by the reaction of liquid silicon with carbon // *J. Amer. Ceram. Soc.* **78**(9), p. 2456-2462 (1995).